Article

SOURCE DATA | TRANSPARENT PROCESS

THE EMBO JOURNAL

Regulation of a transcription factor network by Cdk1 coordinates late cell cycle gene expression

Benjamin D Landry[1,2], Claudine E Mapa[1,2], Heather E Arsenault[1,2], Kristin E Poti[1,2] & Jennifer A Benanti[1,2,*]

Abstract

To maintain genome stability, regulators of chromosome segregation must be expressed in coordination with mitotic events. Expression of these late cell cycle genes is regulated by cyclin-dependent kinase (Cdk1), which phosphorylates a network of conserved transcription factors (TFs). However, the effects of Cdk1 phosphorylation on many key TFs are not known. We find that elimination of Cdk1-mediated phosphorylation of four S-phase TFs decreases expression of many late cell cycle genes, delays mitotic progression, and reduces fitness in budding yeast. Blocking phosphorylation impairs degradation of all four TFs. Consequently, phosphorylation-deficient mutants of the repressors Yox1 and Yhp1 exhibit increased promoter occupancy and decreased expression of their target genes. Interestingly, although phosphorylation of the transcriptional activator Hcm1 on its N-terminus promotes its degradation, phosphorylation on its C-terminus is required for its activity, indicating that Cdk1 both activates and inhibits a single TF. We conclude that Cdk1 promotes gene expression by both activating transcriptional activators and inactivating transcriptional repressors. Furthermore, our data suggest that coordinated regulation of the TF network by Cdk1 is necessary for faithful cell division.

Keywords Cdk1; cell cycle; mitosis; proteolysis; transcription
Subject Categories Cell Cycle; Transcription
DOI 10.1002/embj.201386877 | Received 12 September 2013 | Revised 13 March 2014 | Accepted 17 March 2014 | Published online 8 April 2014
The EMBO Journal (2014) 33: 1044–1060

Introduction

Progression through the cell cycle depends upon the orchestrated expression of hundreds of genes. This cyclical transcription is critical for accurate cell division, as it ensures the proper order of cell cycle events (Haase & Wittenberg, 2014) and prevents uncontrolled proliferation that can lead to the development of cancer (Massagué, 2004). Networks of transcription factors (TFs) control cell cycle-regulated transcription by similar mechanisms in all eukaryotes (Morgan, 2007). Changes in cell cycle-regulated gene expression are further modulated by the activities of cyclin-dependent kinases (CDKs), which can affect both the activity and expression of cell cycle-regulatory TFs.

Cyclin-dependent kinase regulation of transcription is best understood at the G1/S transition, where the properties of transcriptional regulation are conserved from yeast to humans (Cross *et al*, 2011). In late G1, CDK triggers the expression of G1/S genes by directly phosphorylating and inactivating transcriptional repressors (Rb family members in mammals, Whi5 in yeast), which promotes the function of transcriptional activators (E2F in mammals, SBF and MBF in yeast) that stimulate expression of G1/S genes (de Bruin *et al*, 2004; Costanzo *et al*, 2004; van den Heuvel & Dyson, 2008; Henley & Dick, 2012). Later in S-phase, phosphorylation of G1/S activators by S-phase cyclin/CDKs inhibits their function and shuts off gene expression (Bertoli *et al*, 2013). Although CDK also impacts the expression of late cell cycle genes, less is known about the details of this regulation. In budding yeast, genes that peak at the G2/M transition are activated by the forkhead family TF Fkh2 bound to its co-activator Ndd1 and the MADS box protein Mcm1 (Koranda *et al*, 2000; Kumar *et al*, 2000). CDK phosphorylates both Fkh2 and Ndd1 and is required for their interaction and recruitment to target gene promoters (Reynolds, 2003; Pic-Taylor *et al*, 2004). In mammals, the related forkhead protein FoxM1 regulates expression of a similar group of mitotic genes (Laoukili *et al*, 2005), and phosphorylation of the FoxM1 C-terminal transactivation domain by Cdk2 is required for its activity (Major *et al*, 2004; Lüscher-Firzlaff *et al*, 2006; Wierstra & Alves, 2006; Laoukili *et al*, 2008). Thus, the general principles of CDK-regulated transcription are conserved between yeast and mammals throughout the cell cycle.

For many cell cycle-regulatory proteins, CDK phosphorylation not only regulates their activity, but also modulates their expression by stimulating or blocking their ubiquitination and degradation in the proteasome. The activities of the two major families of cell cycle-regulatory ubiquitin ligases, the Skp1-Cullin-F-box (SCF) and anaphase-promoting complex (APC) are both impacted by CDK (Benanti, 2012). Phosphorylation of many cell cycle regulators promotes their interaction with F-box protein subunits of SCF ubiquitin ligases, which leads to their ubiquitination and destruction (Willems *et al*, 2004; Skaar *et al*, 2013). In contrast, CDK phosphorylation of some APC targets near degron motifs inhibits their ubiquitination by the APC (Littlepage & Ruderman,

1 Program in Gene Function and Expression, University of Massachusetts Medical School, Worcester, MA, USA
2 Program in Molecular Medicine, University of Massachusetts Medical School, Worcester, MA, USA
*Corresponding author. Tel: +1 508 856 1773; Fax: +1 508 856 4650; E-mail: Jennifer.Benanti@umassmed.edu

2002; Agarwal *et al*, 2003; Mailand & Diffley, 2005; Holt *et al*, 2008; Ostapenko & Solomon, 2011). As a consequence, CDK phosphorylation limits the expression of cell cycle-regulatory proteins to specific windows of time when their functions are required, thereby reinforcing unidirectional progression through the cell cycle.

Recent studies have demonstrated that cell cycle-regulated transcription is controlled by the coupled activities of a TF network and cyclin/Cdk1 complexes (Orlando *et al*, 2008; Simmons Kovacs *et al*, 2012). Interestingly, almost all cell cycle-regulatory TFs that make up this TF network are directly phosphorylated by Cdk1 (Ubersax *et al*, 2003; Loog & Morgan, 2005; Holt *et al*, 2009; Kõivomägi *et al*, 2011b); however, the details of how phosphorylation regulates the expression and/or activity of many of these TFs have not been examined. In particular, almost nothing is known about how CDK phosphorylation affects a group of four TFs (Hcm1, Tos4, Yox1, and Yhp1) that are expressed together in S-phase and are predicted to impinge upon expression of late cell cycle genes.

To test whether Cdk1 impacts late cell cycle gene expression through regulation of these TFs, we blocked phosphorylation of each of these factors, both individually and simultaneously, and examined the consequences for cell cycle progression and cell cycle-regulated gene expression. Our results demonstrate that Cdk1 drives cyclical gene expression in part through phosphorylation of these TFs. We find that Cdk1 phosphorylation negatively regulates each of these TFs by promoting their degradation. Additionally, we find that phosphorylation is required for the function of the activator Hcm1. Thus, Cdk1 regulates late cell cycle gene expression through the activation of transcriptional activators (Hcm1, Fkh2, and Ndd1) and inactivation of transcriptional repressors (Yox1 and Yhp1). This coordinated positive and negative regulation occurs both on the level of the TF network and on the level of an individual TF, as we demonstrate for Hcm1. Blocking Cdk1-mediated phosphorylation of this TF network results in delayed progression through mitosis and a decrease in overall fitness. Therefore, regulation of transcription by Cdk1 plays an important role in the fidelity of cell division.

Results

Phosphorylation regulates the degradation of S-phase TFs

We focused on four S-phase TFs that are predicted to regulate late cell cycle gene expression and are phosphorylated by Cdk1 (Ubersax *et al*, 2003; Loog & Morgan, 2005; Holt *et al*, 2009; Kõivomägi *et al*, 2011b). Hcm1 is a forkhead family transcriptional activator that induces expression of several mitotic spindle regulators, as well as the downstream TFs Fkh1, Fkh2, and Ndd1 (Pramila *et al*, 2006). Conversely, the repressors Yox1 and Yhp1 function during S-phase to prevent premature expression of genes that are transcribed in G2/M and M/G1 phases. Yox1 and Yhp1 are partially redundant and bind to the same sequence motif, which is found in many promoters that are also regulated by the MADS box protein Mcm1, including a subset of those activated by Fkh2/Ndd1 at the G2/M transition (Pramila *et al*, 2002). Finally, Tos4 was identified as a putative transcriptional regulator that associates with several cell cycle-regulated promoters, including the *FKH2* promoter (Horak *et al*, 2002). Tos4 has also been implicated in transcriptional regulation following DNA damage (de Oliveira *et al*, 2012) and was found to interact with the Rpd3L and Set3c histone deacetylase complexes (Shevchenko *et al*, 2008; de Oliveira *et al*, 2012), suggesting that it acts as a transcriptional repressor, although its molecular function is not known.

To inhibit the phosphorylation of each S-phase TF, we constructed mutants that lack all Cdk1 consensus sites (referred to as Cdk- TFs, see Supplementary Fig S1A for specific mutations). When expressed from a constitutive promoter, these mutations led to increased protein levels of all four TFs (Fig 1A; HA, light exposure) and increased the electrophoretic mobility in a gel (most dramatic for Tos4 and Yhp1), consistent with a loss of phosphorylation (Fig 1A; HA, dark exposure). The observed shifts were similarly reduced upon inhibition of Cdk1, confirming that these shifts are the result of Cdk1 phosphorylation *in vivo*. Moreover, upon comparison to the wild-type TFs, which are all established substrates of Clb2/Cdk1 *in vitro* (Loog & Morgan, 2005; Kõivomägi *et al*, 2011b), we found that the Cdk- TFs showed reduced phosphorylation by Clb2/Cdk1 (Fig 1B, Supplementary Fig S1B), confirming that these mutations eliminate Cdk1 phosphosites.

Each Cdk- TF was then integrated into its endogenous locus and expressed as the sole copy of that TF in the cell. In the course of integrating the stable *YOX1* allele, we found that a more conservative mutation that includes mutations in only the C-terminal S/T-P sites, *yox1-9A*, exhibited phenotypes identical to that of *yox1-13A* (Supplementary Fig S6C). In addition, mutation of this group of C-terminal sites reduced phosphorylation by Cdk1 *in vitro* (Supplementary Fig S1B), confirming that these sites are indeed targeted by Cdk1. Therefore, we integrated this more conservative allele at the endogenous *YOX1* locus. As expected, expression of each wild-type TF increased in S-phase and dropped in mitosis (Fig 1C, Supplementary Fig S2). Notably, expression of each of the Cdk- TFs was prolonged over the course of the cell cycle. This change was most dramatic for Tos4-9A and Hcm1-15A, although Yox1-9A and Yhp1-13A were also expressed at higher levels during G1 and mitosis, as compared to the WT proteins (Fig 1C, see 0 and 60 min time points). We also examined the timing of cell cycle progression in cells expressing each of the Cdk- TFs. None of the mutations significantly altered cell cycle progression under optimal growth conditions, although we noted a subtle, but reproducible, delay in S-phase progression in cells expressing Yox1-9A, compared to WT cells (Supplementary Fig S2).

Phosphorylation by Cdk1 regulates the ubiquitination and degradation of many cell cycle regulators (Benanti, 2012), so we compared the half-lives of wild-type and Cdk- TFs to determine whether phosphorylation affected their stabilities. Each Cdk- TF was more stable than the corresponding WT protein (Fig 1D–G), which accounts for their persistence throughout the cell cycle. Moreover, direct inhibition of Cdk1 similarly stabilized Hcm1, Tos4, and Yox1 (Fig 2A–C), confirming that Cdk1 regulates their stabilities. Interestingly, although Cdk1 inhibition decreased phosphorylation of Yhp1 (Fig 1A), it did not appear to impair Yhp1 degradation (Fig 2D), which could be the result of incomplete Yhp1 dephosphorylation after Cdk1 inhibition. Additionally, we cannot rule out the possibility that some subset of S/T-P sites in each TF are phosphorylated by another kinase *in vivo*. However, our data clearly demonstrate that Cdk1 phosphorylates at least a subset of S/T-P sites in each TF and that phosphorylation of these sites promotes degradation of each factor.

In yeast, most protein degradation that depends upon phosphorylation is triggered by SCF family E3 ubiquitin ligases, especially those containing the F-box proteins Cdc4 or Grr1 that recognize Cdk1-phosphorylated epitopes on substrates (Lanker *et al*, 1996; Nash *et al*, 2001; Kõivomägi *et al*, 2011a; Landry *et al*, 2012; Lyons *et al*, 2013). To determine whether an SCF E3 promotes the degradation of S-phase TFs, we expressed each in cells carrying a temperature-sensitive allele of the core SCF subunit *cdc53-1* and analyzed their degradation upon Cdc53 inactivation. Interestingly, phosphorylated forms of Tos4, Yox1, and Yhp1 were each stabilized in *cdc53-1*

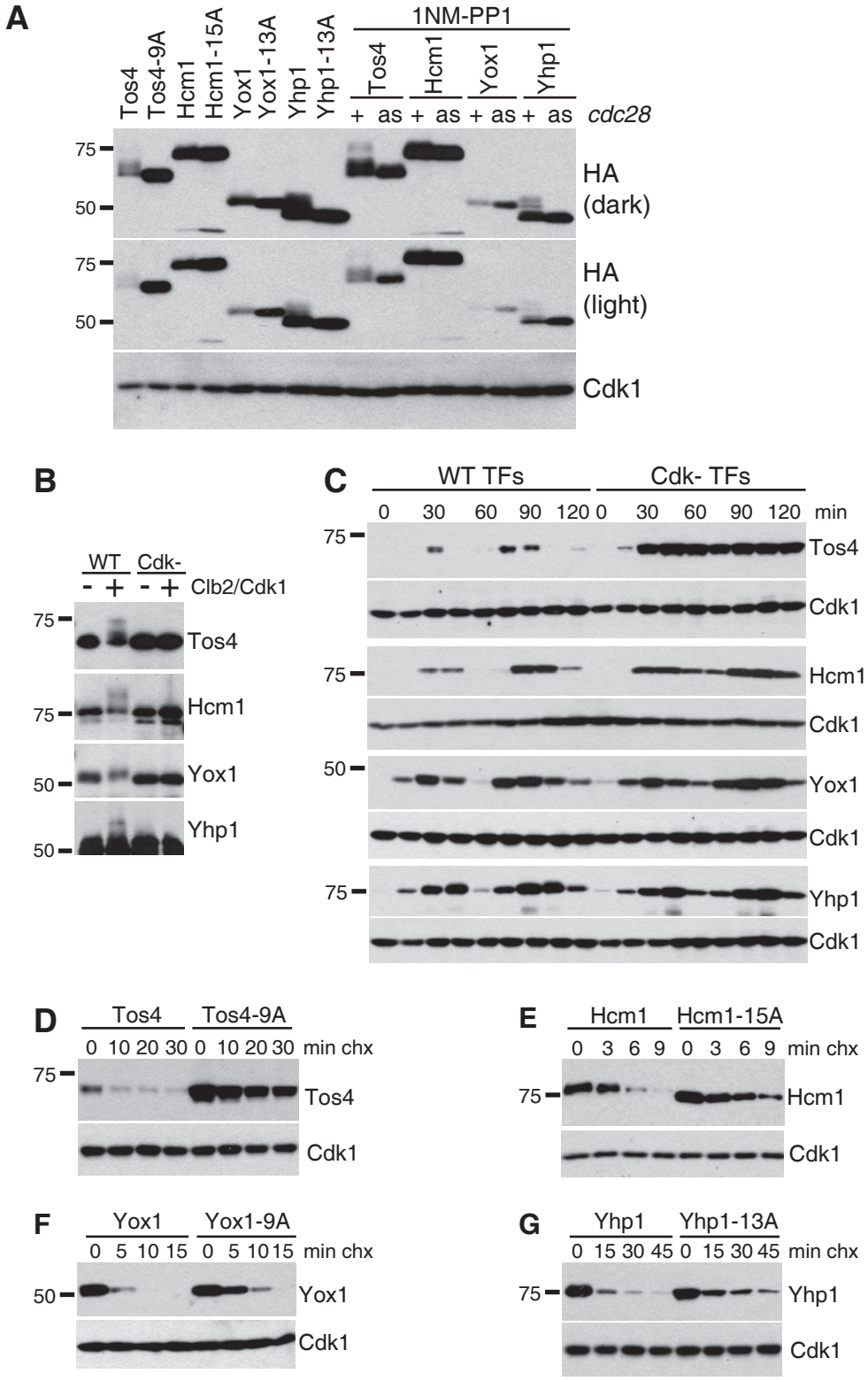

cells (Fig 2E–H), demonstrating that an SCF E3 regulates the degradation of the Cdk-phosphorylated forms of these TFs. Hcm1 was not stabilized in this assay, which could be due to the fact that inactivation of Cdc53 arrests cells in G1 (Supplementary Fig S4B). We subsequently found that Hcm1 degradation in G1 is independent of phosphorylation, but that Hcm1 is targeted by Cdc53 when cells arrested in mitosis (discussed below).

Interestingly, each TF was still degraded to some extent upon blocking phosphorylation (Figs 1D–G and 2A–D) and upon inactivation of the SCF (Fig 2E–H). In addition, Cdk- TFs still undergo modest cell cycle-regulated expression (Fig 1C), suggesting that Cdk-independent pathways also degrade these proteins. One possibility is that they may also be targeted by the APC, since their levels are low in mitosis and G1 when the APC is active. Additionally, some evidence suggests that Yhp1 and Tos4 can be targeted by the APC (Ostapenko & Solomon, 2011; Ostapenko *et al*, 2012), raising the possibility that the APC may promote Cdk-independent degradation of all of these TFs. However, we did not observe any stabilization of Hcm1, Yox1, or Yhp1 in cells lacking the APC activator Cdh1, or in cells in which all APC activity is inhibited by the spindle checkpoint (Fig 2I). In fact, levels of these TFs were lower in *cdh1Δ* cells, most likely because a larger fraction of asynchronous *cdh1Δ* cells are in G2/M when these TFs are not transcribed (Supplementary Fig S4C). As reported previously (Ostapenko *et al*, 2012), Tos4 was partially stabilized in cells lacking the APC activator Cdh1 (Fig 2I). However, upon examination of Tos4 levels in previously described cells in which the core APC subunits are deleted (Thornton & Toczyski, 2003), or in cells in which the APC has been hyperactivated by expression of a constitutively active Cdh1 (Cdh1-m11) (Zachariae *et al*, 1998), we observed no change in Tos4 expression (Fig 2J). This suggests that the Cdk-independent degradation of S-phase TFs is not driven by the APC *in vivo*.

Phosphorylation of S-phase TFs promotes expression of late cell cycle genes

Since all four S-phase TFs are expressed during the same window of the cell cycle (Fig 1C) and are predicted to impact expression of overlapping groups of genes, we reasoned that Cdk1 phosphorylation of these TFs may redundantly regulate gene expression and therefore simultaneous mutation of these TFs may have a larger impact on the cell cycle than any individual allele. For this reason, we introduced all four Cdk- TFs into one strain (referred to as 4P, Fig 3) and analyzed cell cycle progression. In the course of constructing this strain, we found that all combinations of Cdk- TF alleles were viable, including the 4P mutant. The 4P strain expressed each of the four Cdk- TFs at higher levels than its WT counterpart across the cell cycle (Fig 3A), confirming that the Cdk- proteins are expressed similarly when they are integrated individually and all together (compared to Fig 1C). However, in contrast to the single mutant strains, the 4P strain exhibited a delay in progression through mitosis (see 75 and 90 min time points, Fig 3B), consistent with the possibility that expression of mitotic regulatory genes was either reduced or delayed. Interestingly, a similar delay in mitotic progression was also observed in cells lacking all four transcriptional regulators (Supplementary Fig S5B), suggesting that some or all of the phosphosite mutations may impair protein function.

We next examined cell cycle-regulated mRNA levels in the 4P mutant directly, using gene expression microarrays. WT and 4P cells were synchronized in G1 phase, released into the cell cycle, and samples for RNA analysis were collected at 15-min intervals. Work from several laboratories has generated a consensus list of 930 genes that undergo cell cycle-regulated transcription (Cho *et al*, 1998; Spellman *et al*, 1998; Pramila *et al*, 2006; Lu *et al*, 2007). Interestingly, we found that the average expression of these cell cycle-regulated genes was downregulated in S through M phases in 4P cells, while expression during G1 was relatively unaffected (Fig 3C and D, compare 30–75 min time points to 0–15 min time points). We then divided the 930 genes into six groups, based on the timing of their peak expression (Pramila *et al*, 2006), and analyzed average expression of each of these groups of genes at each time point. Peak expression of genes that peak in S-phase and mitosis was downregulated in the first cell cycle after release (Supplementary Fig S5C). Moreover, the average expression of genes that peak in S-phase and are predicted to be targets of Hcm1 was modestly downregulated in 4P cells (Fig 3E), to a similar extent as what has been observed in *hcm1Δ* cells (Pramila *et al*, 2006). Additionally, genes that peak at the M/G1 transition and include Yox1/Yhp1 target genes (Spellman *et al*, 1998; Pramila *et al*, 2002) were similarly downregulated over the cell cycle (Fig 3F). Importantly, although expression of individual genes in these classes continued to cycle (Supplementary Fig S5C and D), their peak expression was reproducibly decreased (Fig 3H). In contrast, *CLB2* cluster genes (Spellman *et al*, 1998), which are regulated by Fkh2/Ndd1 and peak at the G2/M transition (Loy *et al*, 1999; Koranda *et al*, 2000; Kumar *et al*, 2000; Pic *et al*, 2000; Zhu *et al*, 2000), were not significantly altered during the first cell cycle after release (Fig 3G). Decreased expression of *CLB2* cluster genes was observed from 90 to 105 min

Figure 1. Characterization of cyclin-dependent kinase (Cdk)- transcription factors (TF) alleles.

A Wild-type or *cdc28-as1* strains carrying plasmids to express the indicated 3HA-tagged WT or Cdk- TF alleles from the *GAL1* promoter were induced with galactose and levels of HA-tagged proteins compared by Western blot. Where indicated, strains were treated with 1NM-PP1 to inhibit *cdc28-as1* for 10 min prior to collecting cells. Light exposure of the HA blot is shown to highlight changes in levels of Cdk- TFs, and dark exposure highlights the mobility shifts.

B Cells from (A) were arrested in G1 and TF expression induced by galactose addition. TFs were then immunoprecipitated and incubated with or without Clb2/Cdk1 kinase, and phosphorylation analyzed by Western blotting. Note that unphosphorylated Yhp1-3HA co-migrates with IgG.

C Cells expressing Tos4-3FLAG, Tos4-9A-3FLAG, Hcm1-3HA, Hcm1-15A-3HA, Yox1-3V5, Yox1-9A-3V5, Yhp1-13MYC, or Yhp1-13A-13MYC were arrested in G1, released into the cell cycle, and samples taken for Western blot and flow cytometry at 15-min time points. Western blots against epitope tags on WT and Cdk- TFs are shown. Quantification of protein levels and flow cytometry are shown in Supplementary Fig S2.

D–G Cells from (C) expressing tagged WT and Cdk- alleles of Tos4 (D), Hcm1 (E), Yox1 (F), or Yhp1 (G) were treated with cycloheximide and samples collected for Western blot after the indicated number of minutes. For all blots, molecular weight markers are indicated to the left and Cdk1 levels are shown as a loading control. Flow cytometry showing cell cycle positions and quantification of half-life data are shown in Supplementary Fig S3.

Source data are available online for this figure.

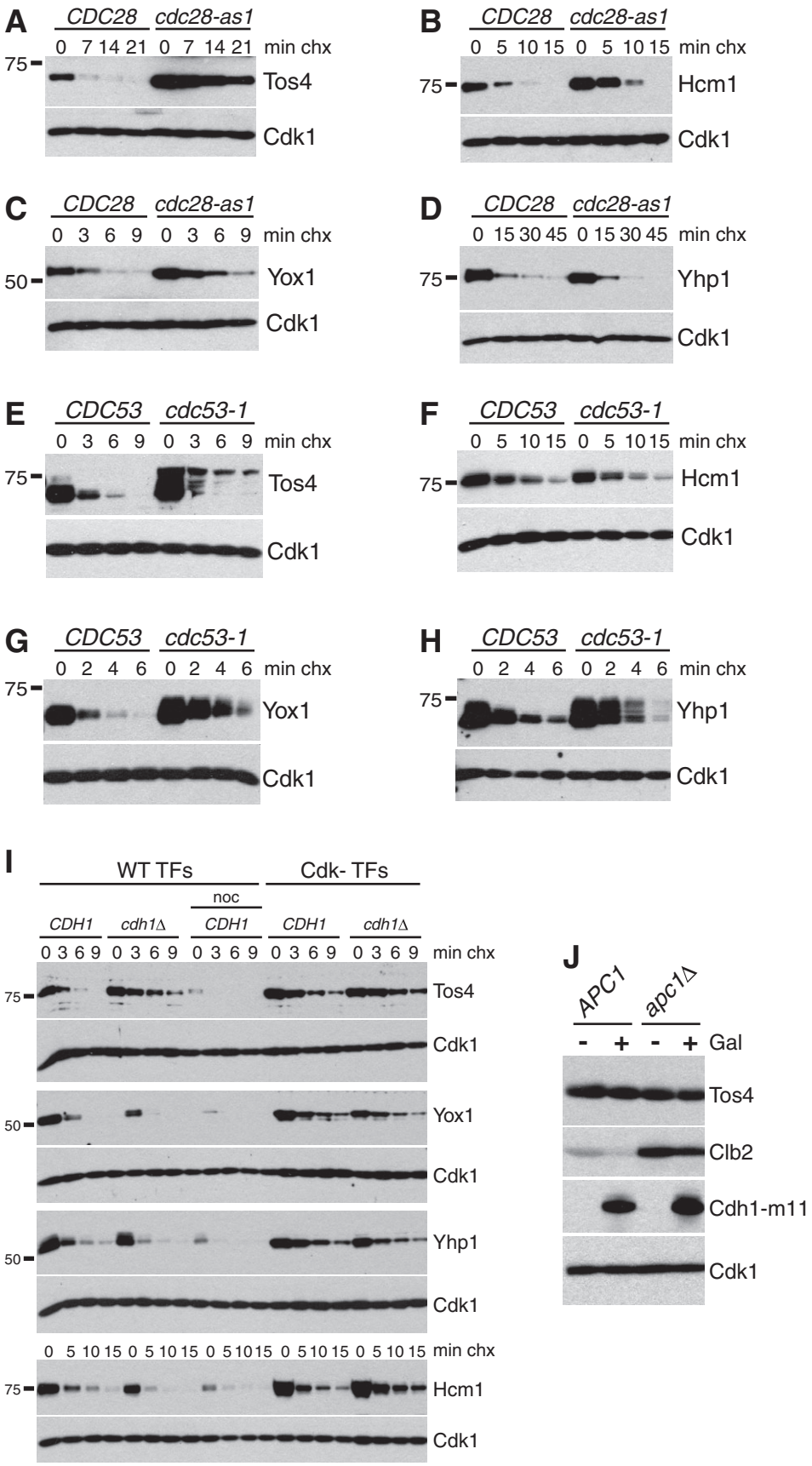

after release, but this is likely due to the fact that 4P cells are delayed in progression through the cell cycle at this time (Fig 3B). Together, this analysis suggests that blocking Cdk1 phosphorylation inhibits the function of the activator Hcm1, and/or increases the activity of the repressors Yox1 and Yhp1, leading to decreased expression of cyclical genes late in the cell cycle.

The repressors Yox1 and Yhp1 are inactivated by phosphorylation

Next, we sought to understand how phosphorylation alters the functions of each individual TF. We first analyzed the consequences of overexpressing each WT and Cdk- TF. Among the four TFs, overexpression of Tos4 or Yox1 has been reported to slow progression through the cell cycle (Pramila *et al*, 2002; de Oliveira *et al*, 2012). However, we found that constitutive overexpression of Tos4 or Tos4-9A had only a very minor effect on growth (Supplementary Fig S6A). Tos4 has also been implicated in the DNA damage response due to the fact that deletion of *TOS4* and the checkpoint kinase *DUN1* was found to be synthetic lethal in the presence of the replication inhibitor hydroxyurea (HU) (de Oliveira *et al*, 2012). We attempted to reproduce this finding, using *tos4Δ* cells, in order to test whether *tos4-9A* showed a similar genetic interaction with *dun1Δ*, but could not replicate the reported result for *tos4Δ* (Supplementary Fig S6B). Because of the lack of phenotypes in these assays, we did not investigate the molecular consequences of phosphorylation on Tos4 further.

In contrast to *TOS4*, *YOX1* overexpression severely impaired growth and, interestingly, overexpression of *yox1-13A* was even more deleterious, suggesting that it is a hyperactive allele (Supplementary Fig S6A). To determine whether Yox1 or Yox1-13A arrested cells in a specific cell cycle phase, cells were arrested in G1 and overexpression was induced as cells were released from the arrest. Notably, *yox1-13A* overexpression led to a mitotic arrest, which did not occur upon overexpression of WT *YOX1* (Fig 4A). Since Yox1-13A was expressed at higher levels than WT Yox1 (Fig 4B), this raised the possibility that it blocked cell cycle progression due to increased repression of target genes. Indeed, expression of four targets (*DBF2*, *HST4*, *MCM3*, and *CDC20*) was reduced following overexpression of WT Yox1, and to a greater extent following overexpression of Yox1-13A (Fig 4C). Interestingly, the differences in target gene expression between WT and 13A-overexpressing cells were relatively modest, yet only the 13A-overexpressing cells arrested in mitosis. This suggests that a small increase in expression of these mitotic genes is sufficient to promote cell cycle progression.

We next examined whether blocking phosphorylation of endogenous Yox1 had a similar effect on gene expression. Since mutation of 9 C-terminal sites of Yox1 (Supplementary Fig S1A) was sufficient to confer both cell cycle arrest and decreased target gene expression upon overexpression (Supplementary Fig S6C, unpublished observations), the *yox1-9A* allele was integrated into the genomic locus and used for further analysis. Additionally, since Yhp1 and Yox1 are related proteins that regulate overlapping sets of genes (Pramila *et al*, 2002), we also analyzed *yhp1-13A*. Notably, Yox1/Yhp1 target genes that peak in M/G1, including *DBF2*, *HST4*, *KIN3*, and *MCM3*, were downregulated in *yox1-9A*, *yhp1-13A*, and double-mutant cells (Fig 4D). In contrast, the Yox1 target genes *CDC20* and *SPO12*, which peak earlier in G2/M (Pramila *et al*, 2002; Darieva *et al*, 2010), were not greatly affected. Consistent with the downregulation of M/G1 genes, Yhp1-13A and Yox1-9A also associated with the promoters of these genes at higher levels than the wild-type proteins (Fig 4E). Interestingly, mutation of Cdk1 sites had greater effects on DNA binding of Yox1 than on Yhp1, which could be due to the larger increase in Yox1 protein levels that are observed upon mutation of Cdk sites (Supplementary Fig S7B). Together, these data further support the model that Cdk1 phosphorylation normally promotes degradation of Yox1 and Yhp1, thereby restricting the activity of these transcriptional repressors to S-phase.

Phosphorylation of the Hcm1 N-terminus promotes its degradation

Surprisingly, although the Hcm1-15A mutant was more stable than WT Hcm1 (Fig 1C), Hcm1 target genes were downregulated in 4P cells (Fig 3E), suggesting that Hcm1-15A might be less active than WT Hcm1. To determine whether these opposing effects of phosphorylation on Hcm1 could be uncoupled, we mutated different subsets of its phosphosites. The 15 Cdk1 consensus sites in Hcm1 primarily cluster in two groups outside of the DNA-binding domain, with three sites in the N-terminus and eight in the C-terminus (Supplementary Fig S1A). To dissect the functions of each cluster, we first examined whether each can be targeted by Cdk1. Importantly, Hcm1 proteins containing only the 3 N-terminal S/T-P sites (Supplementary Fig S1B, Hcm1-12C), or only the 8 C-terminal sites (Hcm1-7N), were phosphorylated by Cdk1 *in vitro*, but to lesser degrees than the wild-type protein that contains all sites, confirming that some sites in each cluster are targeted. We then constructed two additional mutants that contained Ser/Thr to Ala mutations in only the three N-terminal sites (referred to as 3N) or the 8 C-terminal

Figure 2. Regulation of transcription factors (TF) degradation.

A–D Regulation of TF degradation by cyclin-dependent kinase 1 (Cdk1). Cells carrying the *cdc28-as1* allele (or wild-type controls) and expressing Tos4-3FLAG (A), Hcm1-3HA (B), Yox1-3V5 (C), or Yhp1-13MYC (D) were treated with 1NM-PP1 for 2 h and half-lives compared by cycloheximide-chase assay. Flow cytometry controls showing cell cycle positions are shown in Supplementary Fig S4A.

E–H Cells carrying the *cdc53-1* temperature-sensitive allele (or wild-type controls), and expressing Tos4-3HA (E), Hcm1-3HA (F), Yox1-3HA (G), or Yhp1-3HA (H) from the inducible *GAL1* promoter on plasmids, were treated with galactose for 30 min, shifted to 37°C for 2 h, and cycloheximide-chase assays was performed. Note that for Tos4, Yox1, and Yhp1, phosphorylated forms of each are stabilized in *cdc53-1* cells. Flow cytometry controls showing cell cycle positions are shown in Supplementary Fig S4B.

I Cycloheximide-chase assay comparing the half-lives of HA-tagged WT and Cdk- alleles (integrated at the endogenous locus) in wild-type cells to cells deleted for the anaphase-promoting complex (APC) activator Cdh1, or arrested with nocodazole. Flow cytometry profiles for each strain are shown in Supplementary Fig S4C.

J Wild-type and *apc1Δ* strains were treated with galactose to induce expression of constitutively active Cdh1 (Cdh1-m11) and levels of Tos4-3FLAG, Cdh1-m11, Clb2 (an established APC target), and Cdk1 were analyzed by Western blotting.

Source data are available online for this figure.

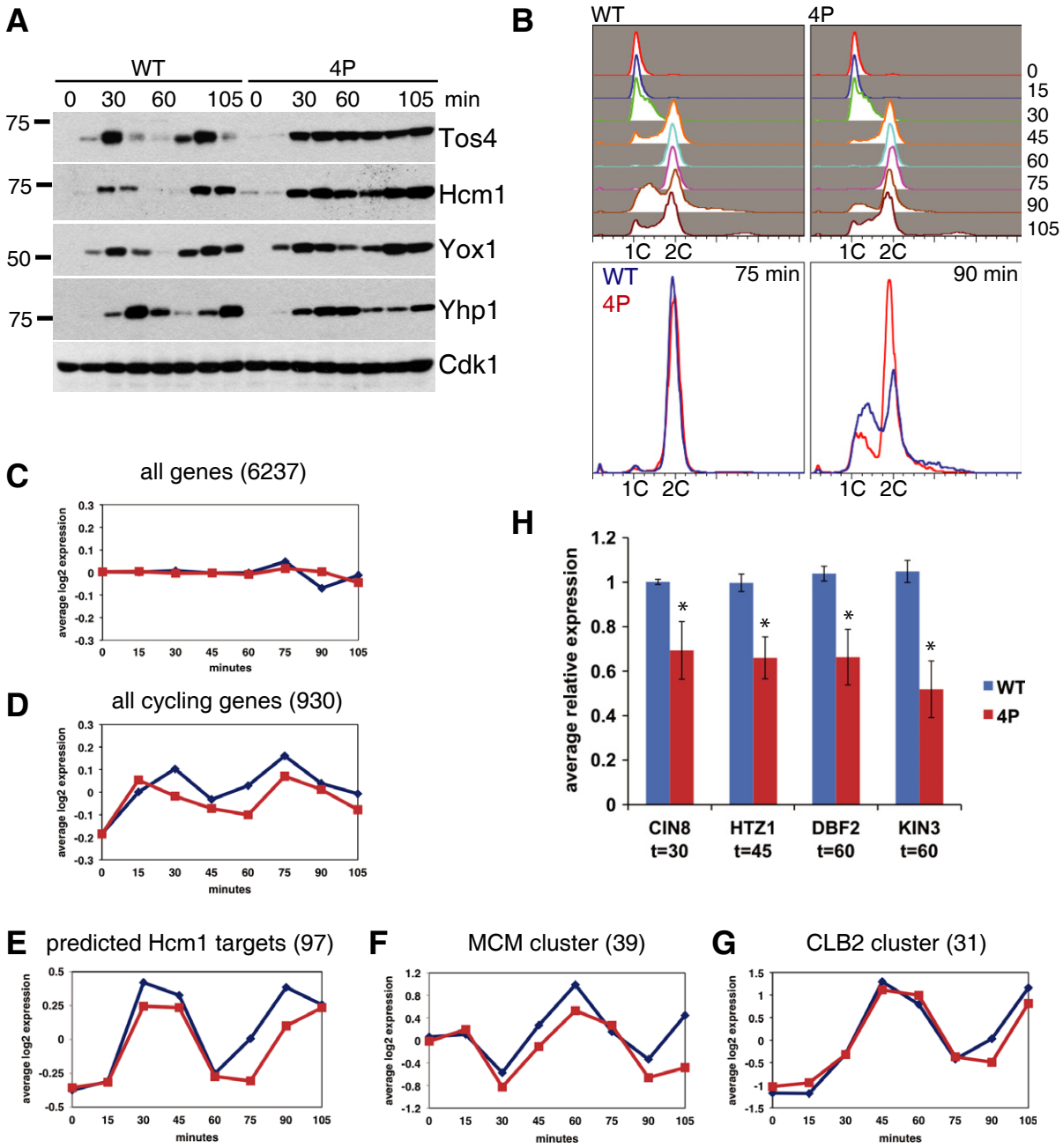

Figure 3. Simultaneous mutation of S-phase transcription factors (TFs) delays mitotic progression.

A, B Cells expressing differentially tagged WT TFs (*TOS4-3FLAG HCM1-3HA YOX1-3V5 YHP1-13MYC*), or phosphomutant TFs (4P, *tos4-9A-3FLAG hcm1-15A-3HA yox1-9A-3V5 yhp1-13A-13MYC*), were arrested in G1, released, and collected at 15-min intervals for Western blot (A) and flow cytometry (B). Levels of TFs and cyclin-dependent kinase 1 (Cdk1) are shown in (A). Quantification of proteins levels are shown in Supplementary Fig S5A. DNA content at each time point is shown (B, top). Overlay of WT (blue) and 4P (red) at 75 and 90 min highlight the mitotic delay in 4P cells (B, bottom). A representative of three replicate experiments is shown.

C–G mRNA from WT and 4P cells collected as in (A) were compared to mRNA from asynchronous WT cells. Data from one of two biological replicates are shown. Average expression of all 6,237 genes at each time point in WT (blue) and 4P (red) cells (C). Average expression of 930 cell cycle-regulated genes (D). For further explanation and breakdown of individual groups, see Supplementary Fig S5C. Average expression of 97 genes that have Hcm1-binding motifs in their promoters and whose expression peaks during S-phase (E) (Pramila *et al*, 2006). Average expression of 39 MCM cluster genes (F) (Spellman *et al*, 1998). Average expression of 31 *CLB2* cluster genes (G) (Spellman *et al*, 1998). Data from biological replicates of all cell cycle-regulated genes, and lists of genes in each cluster, are included in Supplementary Dataset S1.

H RT-qPCR of representative Hcm1 targets (*CIN8*, *HTZ1*) and MCM cluster genes (*DBF2*, *KIN3*) at the indicated time points after release from G1. For each gene, mean expression from three biological replicates, with standard deviations, is plotted. Asterisks indicate that all four comparisons are statistically significant with a *P*-value of ≤ 0.01 (*CIN8*, $P = 0.01$; *HTZ1*, $P = 0.005$; *DBF2*, $P = 0.007$; *KIN3*, $P = 0.003$).

Data information: In all parts, wild-type cells are graphed in blue, 4P cells are red.
Source data are available online for this figure.

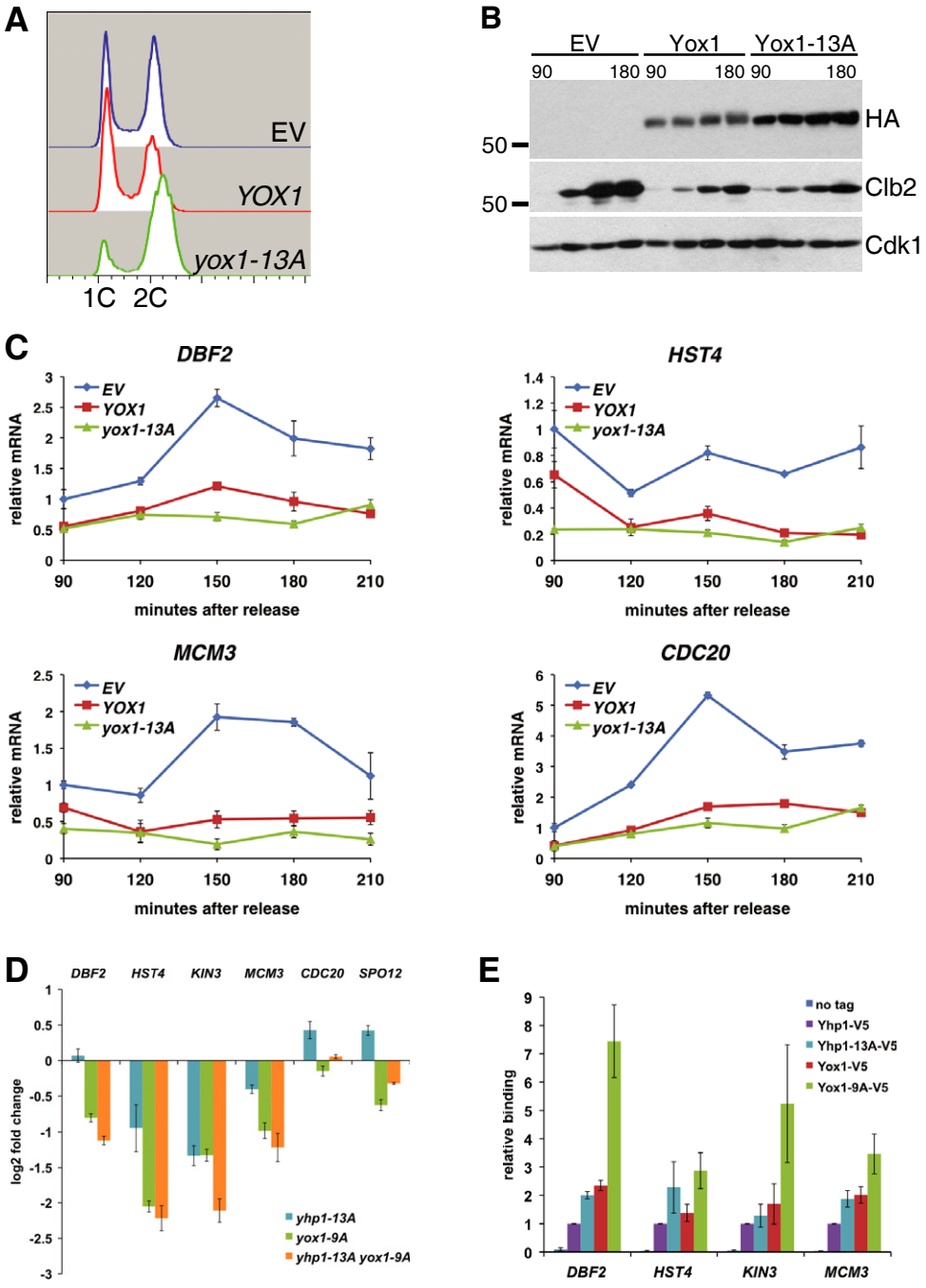

Figure 4. Phosphorylation inactivates Yox1 and Yhp1.

A–C Wild-type cells carrying plasmids expressing *YOX1* or *yox1-13A* from the *GAL1* promoter, or an empty vector control (EV), were grown in raffinose and arrested in G1. Cells were then released into medium containing raffinose and galactose, to induce overexpression of *YOX1* or *yox1-13A*. DNA content 5 h after release from G1 is shown in (A). Western blots for Yox1-3HA, Clb2 (a marker of mitosis), and cyclin-dependent kinase 1 (Cdk1; loading control) as cells progressed through mitosis (90, 120, 150, and 180 min after release from G1) are shown in (B). Expression of the Yox1 target genes *DBF2*, *HST4*, *MCM3*, and *CDC20* at the indicated time points is shown in (C). All values were normalized to *ACT1*. Mean and standard deviations from technical replicates of a representative experiment are shown. For each gene, values are shown relative to empty vector control cells at 90 min after release. Flow cytometry profiles for all time points are shown in Supplementary Fig S7A.

D Expression of Yox1/Yhp1 targets genes in asynchronous *yhp1-13A*, *yox1-9A*, or *yhp1-13A yox1-9A* cells compared to wild-type. All values were normalized to *ACT1*. Mean and standard deviations from technical replicates of a representative experiment are shown. See Supplementary Fig S7B and C for corresponding Western blots and cell cycle positions.

E ChIP-qPCR of 3V5-tagged Yhp1, Yhp1-13A, Yox1, and Yox1-9A, compared to an untagged control. Mean and standard deviations for three biological replicates are shown. For each primer set, binding is shown relative to Yhp1. See Supplementary Fig S7C and D for corresponding Western blots and cell cycle positions from a representative experiment.

Source data are available online for this figure.

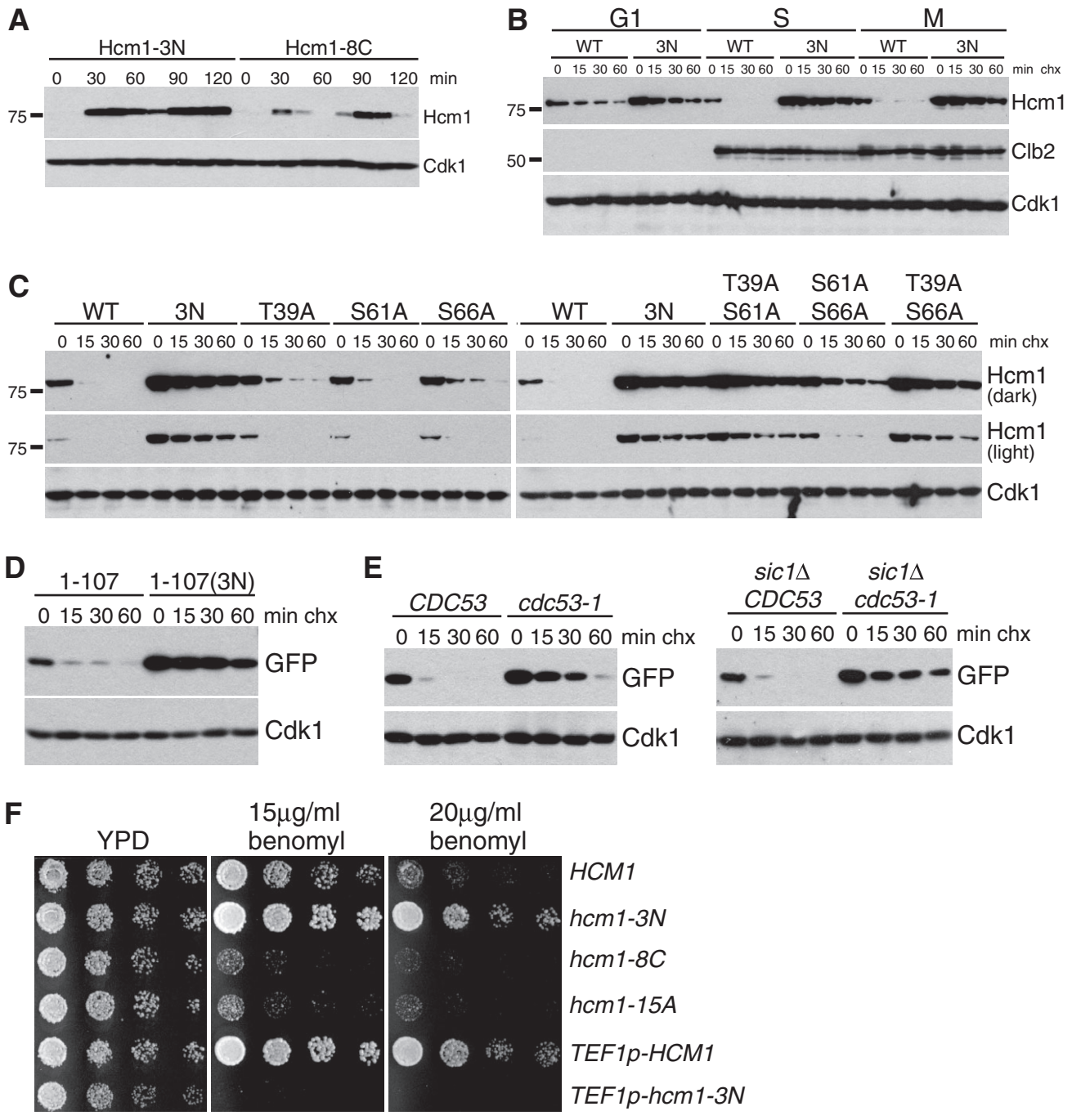

Figure 5. Phosphorylation of the Hcm1 N-terminus promotes SCF-dependent degradation.

A Expression of Hcm1-3N-3HA and Hcm1-8C-3HA over the cell cycle. Cells were arrested in G1, released into the cell cycle, and samples taken for Western blot and flow cytometry (Supplementary Fig S8A) at 15-min time points.

B Cells expressing Hcm1-GFP or Hcm1-3N-GFP from the *TEF1* promoter were arrested in G1 with alpha-factor, S-phase with HU, or mitosis with nocodazole and half-lives compared by cycloheximide-chase assay. Levels of Hcm1, Clb2, and cyclin-dependent kinase 1 (Cdk1) are shown. Cell cycle arrest was confirmed by flow cytometry (Supplementary Fig S8B).

C Cells expressing the indicated Hcm1 mutants from the *TEF1* promoter were arrested in mitosis (Supplementary Fig S8C) and half-lives compared by cycloheximide-chase assay. Two exposures of Hcm1 blots are shown to highlight differences in stability between the double phosphomutants.

D Cycloheximide-chase assay of Hcm1(1-107)-GFP and Hcm1(1-107)3N-GFP fusion proteins in asynchronous cells.

E *CDC53*, *cdc53-1*, *sic1Δ CDC53*, and *sic1Δ cdc53-1* cells expressing Hcm1(1-107)-GFP were arrested in mitosis (Supplementary Fig S8D) at the permissive temperature, shifted to 37°C for 15 min, and half-lives compared by cycloheximide-chase assay.

F Fivefold dilutions of cells with the indicated genotypes were spotted onto rich medium plates (YPD), or plates containing the indicated concentrations of benomyl.

Source data are available online for this figure.

sites (referred to as 8C). Interestingly, Hcm1-3N expression was increased over the cell cycle, as with the Hcm1-15A allele, whereas Hcm1-8C was expressed in a pattern similar to WT Hcm1 (Fig 5A, compared to Fig 1C). To gain further evidence that Cdk1 mediates Hcm1 degradation by phosphorylating these three N-terminal sites, we examined turnover of Hcm1 in cell cycle phases that have different levels of Cdk1 activity. Because *HCM1* is only transcribed in S-phase, the constitutive *TEF1* promoter was introduced upstream of the *HCM1* gene, so that it would be expressed throughout the cell cycle. Notably, in S and M phases, when Cdk1 activity is high (as confirmed by high Clb2 levels, Fig 5B), Hcm1 was rapidly degraded in a manner dependent upon the three Cdk1 consensus sites in the N-terminus (Fig 5B). In contrast, the half-life of Hcm1 was longer in G1-arrested cells that lack Cdk activity, and the degradation that did occur was independent of the three phosphosites (Fig 5B). This confirms that Hcm1 is degraded by a Cdk1-dependent pathway.

To gain a better understanding of how Hcm1 degradation is regulated, we next sought to identify the specific sites within the N-terminus that are required for its degradation. Interestingly, mutation of no single site stabilized Hcm1; however, mutation of T39 and either of the remaining two sites (S61 or S66) was sufficient to almost completely stabilize the protein (Fig 5C), supporting the model that multiple phosphorylations are required for optimal degradation. Additionally, we found that the first 107 amino acids of Hcm1 constitutes a transferrable degron: This sequence promoted degradation of GFP when fused to its N-terminus, in a manner dependent upon the three Cdk1 consensus sites (Fig 5D).

Interestingly, although earlier experiments examining full-length Hcm1 (Fig 2F) suggested that Hcm1 degradation was not altered upon inactivation of the core SCF subunit Cdc53, we noted that the arrangement of Cdk1 consensus sites in the Hcm1 N-terminus resembled a phosphodegron recognized by the F-box protein Cdc4 (Hao *et al*, 2007; Kõivomägi *et al*, 2011a). We considered the possibility that SCF-mediated degradation was masked in earlier experiments due to the fact that *cdc53-1* cells arrest in G1, when degradation occurs independent of N-terminal phosphorylation (Fig 5B). Consistent with this possibility, Hcm1(1-107)-GFP was stabilized in *cdc53-1* cells that were arrested in mitosis (Fig 5E). Moreover, this stabilization was also observed in cells lacking the Cdk1 inhibitor Sic1, confirming that the stabilization was not an indirect consequence elevated Sic1 and inhibition of Cdk1 activity. Together, these data support the model that, like the other S-phase TFs, the Cdk1-dependent degradation of Hcm1 is mediated by an SCF ubiquitin ligase.

Next, we tested whether Hcm1-3N or Hcm1-8C showed reduced activity as a transcriptional activator, as we observed for Hcm1-15A. First, we examined the growth of each strain on media containing the microtubule destabilizing drug benomyl. Although benomyl sensitivity may be an indirect consequence that results from a general disruption of mitotic gene expression, earlier studies found that *hcm1Δ* cells are benomyl-sensitive which makes this a straightforward measure of Hcm1 activity (Pramila *et al*, 2002; Daniel *et al*, 2006). Cells expressing Hcm1-15A or Hcm1-8C were similarly sensitive to benomyl (Fig 5F), suggesting that both are loss-of-function alleles. In contrast, overexpression (*TEF1p-HCM1*) or stabilization (*hcm1-3N*) of Hcm1 led to enhanced benomyl resistance, consistent with the fact that these cells have increased Hcm1 activity. Interestingly, overexpression of stable Hcm1 (*TEF1p-hcm1-3N)* had the opposite effect compared to overexpression or stabilization alone, resulting in benomyl hypersensitivity. Thus, just as having too little Hcm1 sensitizes cells to benomyl, overproduction of Hcm1 (and/or misexpression at inappropriate times in the cell cycle) is detrimental when spindle function is compromised. These data suggest that the transcriptional program that is driven by Hcm1 is important for fine-tuning the sensitivity of the spindle checkpoint response.

Phosphorylation of the C-terminus of Hcm1 is required for its activity

Since Hcm1 targets were downregulated in 4P cells (Fig 3E), and cells expressing either Hcm1-15A or Hcm1-8C were sensitive to benomyl (Fig 5F), this suggested that Cdk1-dependent phosphorylation of the C-terminus of Hcm1 may be required for its activity. To test this directly, we examined expression of several Hcm1 target genes during S-phase and found that they were downregulated in *hcm1-15A* and *hcm1-8C* cells, as in *hcm1Δ* cells (Fig 6A). One trivial possibility is that changing Ser/Thr residues in the C-terminus leads to misfolding of Hcm1 and that the 8C mutant is non-functional for this reason. Therefore, to provide further evidence that phosphorylation of the Hcm1 C-terminus is important for its function, we attempted to construct a phosphomimetic version of the protein. First, all 8 C-terminal Ser/Thr residues were changed to Glu (Hcm1-8E). Cells expressing this mutant grew slightly better than *hcm1-8C* cells on benomyl plates, but were more sensitive than WT cells (Fig 6B). One possible explanation for this partial effect may be that a phosphorylated Ser or Thr introduces a change in net charge of −2, whereas the replacement of a Ser/Thr with a single Glu only changes the net charge by −1. Previously, substitution with two Glu residues was shown to more closely mimic the phoshphorylated state than individual Glu replacements (Strickfaden *et al*, 2007), so we used a similar strategy and replaced Ser/Thr-Pro motifs with Glu-Glu in the Hcm1 C-terminus (Hcm1-16E). Interestingly, *hcm1-16E* cells were substantially healthier on benomyl plates than *hcm1-8C* cells and were comparable to wild-type cells (Fig 6B). We then examined target gene expression in *hcm1-16E* cells and found only modest changes in gene expression, compared to the *hcm1-8C* mutant (Fig 6A). These data support the model that increasing the negative charge of the Hcm1 C-terminus through phosphorylation is important for its activity, perhaps by mediating interactions with other regulatory proteins.

Next, we investigated how phosphorylation regulates Hcm1 activity. First, we examined Hcm1 localization, since the subcellular localization of some forkhead TFs is regulated by phosphorylation (Myatt & Lam, 2007). However, nuclear localization of Hcm1 was not disrupted by any of the Cdk1 site mutations, although the stabilized forms (Hcm1-15A and Hcm1-3N) were detectable throughout the cell cycle instead of being restricted to S-phase cells (Supplementary Fig S9). We then tested whether modulating the phosphorylation of the Hcm1 C-terminus affected its recruitment to target gene promoters. Interestingly, the association of Hcm1-8C with several target promoters was strongly reduced relative to WT, whereas the Hcm1-16E phosphomimetic mutant was recruited slightly better than wild-type (Fig 6C). Thus, Cdk1 phosphorylation appears to promote the activity of Hcm1 by stimulating its association with chromatin. Altogether, our data indicate that Cdk1 phosphorylation has two opposing effects on Hcm1: Phosphorylation of the C-terminus

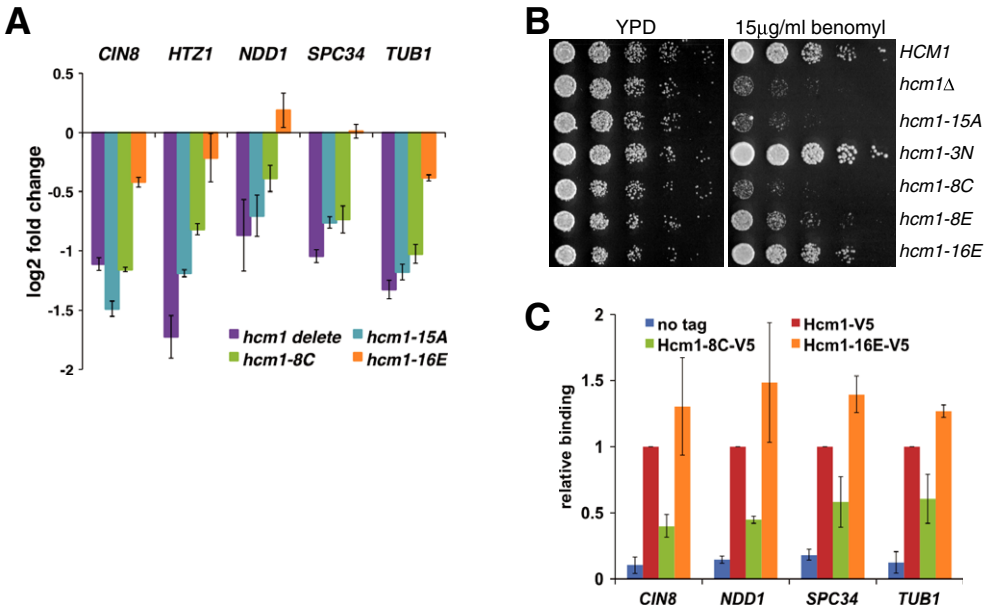

Figure 6. Phosphorylation of the C-terminus of Hcm1 is required for activity.

A Cells with the indicated genotypes were synchronized in late S-phase by arresting in G1 and collecting 45 min after release (Supplementary Fig S10A). Expression of target genes was compared by RT-qPCR. All values are normalized to *ACT1* and shown relative to Hcm1 WT cells. Mean and standard deviations from technical replicates of a representative experiment are shown.

B Fivefold dilutions of cells with the indicated genotypes were spotted onto rich medium plates (YPD), or plates containing 15 μg/ml benomyl.

C ChIP-qPCR of V5-tagged Hcm1, Hcm1-8C, Hcm1-16E, and an untagged control from cells that were arrested in G1 and collected 37 min after release (Supplementary Fig S10B). Mean and standard deviations from three biological replicates are shown. For each primer set, binding is shown relative to Hcm1 wild-type.

promotes its DNA binding activity, leading to activation of its target genes, while phosphorylation of the N-terminus leads to its degradation.

Coordinated phosphorylation of S-phase TFs is important for cellular fitness

Our analyses of individual TFs led to the model that Cdk1 promotes expression of late cell cycle genes by stimulating the activity of a transcriptional activator (Hcm1) and inactivating transcriptional repressors (Yox1, Yhp1) in S-phase. We hypothesized that phosphorylation by Cdk1 might be necessary to coordinate the activities of these TFs, in order to ensure that their target genes are expressed in the proper order as cells progress through S-phase and mitosis. To gain a better understanding of the importance of this regulation, we took a genetic approach and examined a panel of strains that includes every possible combination of Cdk- TF alleles.

First, we measured the median cell size of each strain in an asynchronous cell culture, since subtle differences in proliferation rates often lead to differences in the median size of a population (Jorgensen *et al*, 2002). Interestingly, the 4P strain (*hcm1-15A tos4-9A yox1-9A yhp1-13A*) was approximately 17% larger than a matched wild-type strain (48.5 fL compared to 41.45 fL, Fig 7A). The size of this strain is comparable to what have been classified as large mutants among the collection of non-essential gene deletion strains (the largest 5%) (Jorgensen *et al*, 2002). Among the single mutant Cdk-TF strains, *hcm1-15A* had the largest change in cell size, whereas the other single mutants were larger than wild-type, but smaller than *hcm1-15A* (Fig 7A). Notably, combining any second mutation with *hcm1-15A* increased the size to a level comparable to the 4P strain, and any subsequent mutations did not increase size further, suggesting that the other TFs may impinge upon the same cellular processes.

Since combining any second mutation with *hcm1-15A* led to a further increase in cell size, we hypothesized that the inclusion of other Cdk- TFs may also exacerbate the benomyl sensitivity of *hcm1-15A* cells. Surprisingly, in contrast to *hcm1-15A*, the 4P strain grew as well as wild-type on benomyl plates, as did a triple mutant that included both *yox1-9A* and *yhp1-13A* alleles (Fig 7B). However, *yox1-9A* or *yhp1-13A* alone could not rescue the *hcm1-15A* phenotype. These results suggest that hyperactivation of Yox1/Yhp1 counteracts the consequences of Hcm1 loss of function in this scenario. A likely possibility is that the decreased expression of Yox1/Yhp1 target genes slows progression through mitosis, thereby allowing cells to cope with the compromised spindle function that occurs in *hcm1-15A* cells when they are challenged with benomyl (see further discussion below).

We observed a similar relationship between *hcm1-15A* and the other Cdk- TFs in a fitness assay. Strains of different genotypes were co-cultured and the fraction of each strain in the culture was quantified over time. In this assay, *hcm1-15A* mutants exhibited a strong fitness defect, whereas a strain carrying the other three Cdk- alleles (3P, *tos4-9A yhp1-13A yox1-9A*) was as fit as wild-type (Fig 7C). Interestingly, similar to the benomyl result, the *hcm1-15A* fitness defect was partially rescued in the 4P strain that included all four Cdk- TFs. However, it is important to note that although it was healthier than the *hcm1-15A* strain, the 4P mutant was less fit than wild-type. This is consistent with the observation that 4P cells have

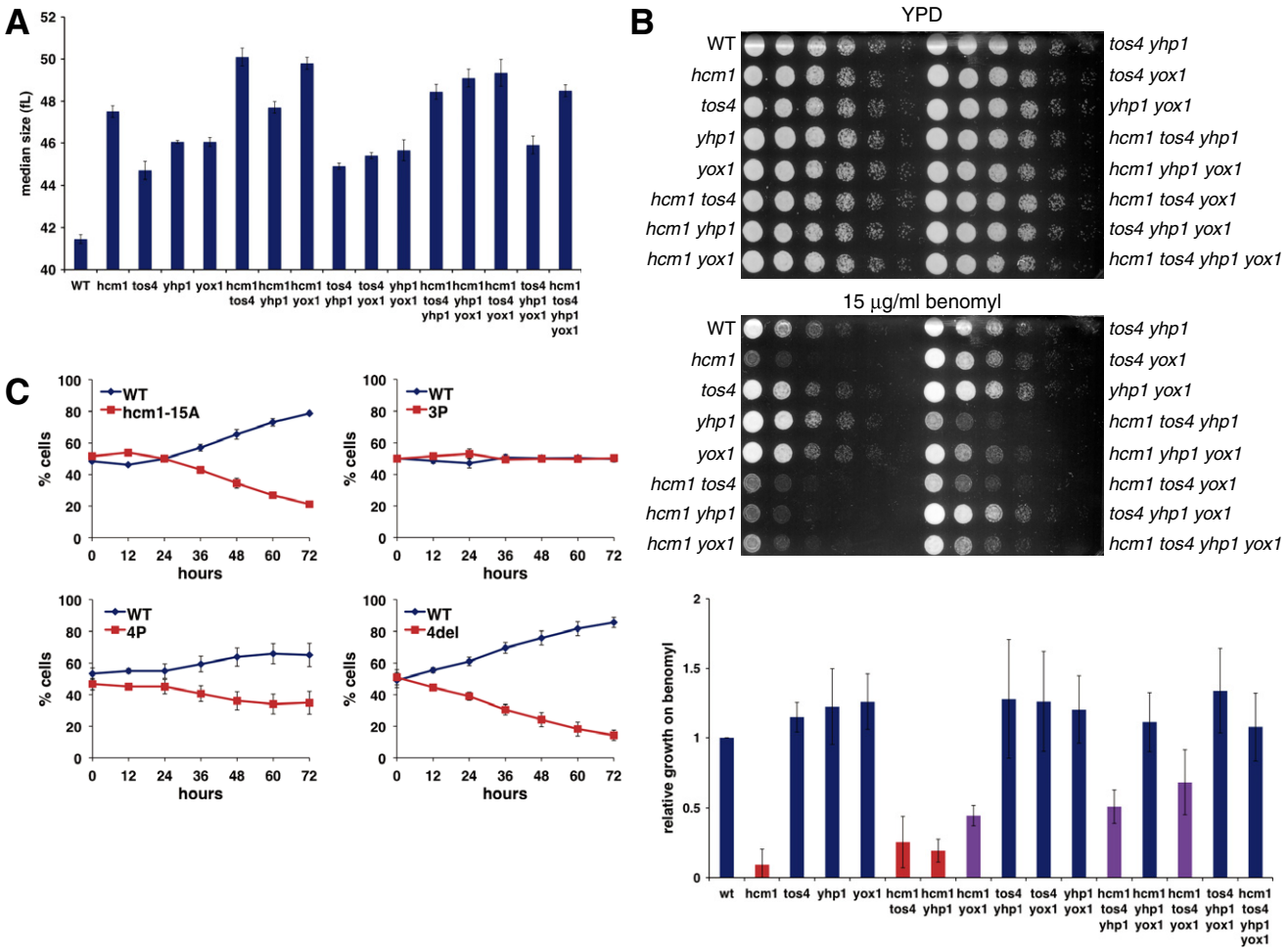

Figure 7. Coordinated phosphorylation of S-phase transcription factors (TFs) is important for fitness.

A Median cell volume of asynchronous cultures carrying cyclin-dependent kinase (Cdk)- mutations in the indicated TFs. The mean and standard deviations from three independent experiments are graphed.

B Fivefold dilution of cells from (A) were spotted onto rich medium plates (YPD), or plates containing 15 μg/ml benomyl (top). Growth on benomyl plates (at a sub-saturating dilution) was quantified with ImageJ and normalized to growth on YPD. Mean and standard deviations of relative growth from three independent experiments are graphed (bottom). Benomyl sensitive (red bars), wild-type sensitivity (blue bars), intermediate sensitivity (purple bars).

C The percentage of cells in co-cultures of strains carrying *PGK1-URA3* (blue lines) and *PGK1-GFP-URA3* (red lines) were determined at the indicated time points. 4P, *hcm1-15A tos4-9A yox1-9A yhp1-13A*; 3P, *tos4-9A yox1*-9A *yhp1-13A*; 4del, *hcm1Δ tos4Δ yox1Δ yhp1Δ*. Mean and standard deviations of 4–6 experiments are shown.

a delay in mitosis when growing exponentially (Fig 3B) and confirms that Cdk1 phosphorylation of these TFs is important for overall fitness. Importantly, losing phosphorylation of these TFs is not equivalent to deleting all four TFs, since a more severe defect was observed in a quadruple delete strain (Fig 7C). These results highlight the utility of dissecting phosphorylation networks using a combinatorial genetic analysis. Additionally, these findings illustrate how Cdk1 acts as a master regulator of S/M-phase transcription, by coordinately regulating the activities of TFs that collectively control the expression of late cell cycle genes.

Discussion

Although Cdk1 is known to be required for robust regulation of cell cycle-regulated gene expression (Orlando *et al*, 2008; Simmons Kovacs *et al*, 2012), the mechanism by which it controls the TF network is not well understood. Here, we have elucidated this regulation by directly eliminating phosphorylation of four TFs that are co-expressed in S-phase. Interestingly, mutation of no individual S-phase TF significantly impacted the cell cycle (Supplementary Fig S2A, C, E and G). However, when Cdk1 phosphorylation of all four TFs was eliminated simultaneously, cells showed decreased expression of late cell cycle genes (Fig 3C–H), progressed through mitosis at a slower rate (Fig 3B), and had reduced fitness (Fig 7C), confirming the overall importance of Cdk1 regulation of this group of S-phase TFs.

The mitotic delay that we observed in 4P cells is most likely due to the widespread reduction of genes that are required for progression through mitosis. Interestingly, most cell cycle-regulated genes continue to cycle in 4P cells, similar to what is observed in cells that lack all Cdk1 activity (Haase & Reed, 1999; Orlando *et al*, 2008).

However, we find that many late cell cycle genes never reach maximal expression (Fig 3, Supplementary Fig S5C and D). During S-phase, Hcm1 activates transcription of a large number of genes that impact chromosome segregation and the mitotic spindle (Pramila *et al*, 2006). Conversely, Yox1 and Yhp1 act in S-phase to prevent premature expression of genes that promote the M/G1 transition. Thus, the combination of reduced Hcm1 activity and increased Yox1/Yhp1 function in 4P cells appears to lead to reduced expression of both groups of genes, and slower progression through mitosis. Interestingly, while this combination of mutations slows the cell cycle and leads to decreased fitness under optimal growth conditions, the coordinate downregulation of both groups of target genes may actually be beneficial to cells when they are challenged with spindle disruption. By slowing progression through mitosis, the hyperactivation of Yox1 and Yhp1 may help cells cope with the compromised spindle function that occurs in the absence of Hcm1 activity.

Previous results suggested that mutation of each of the four TFs would impact the expression and function of the downstream TFs Fkh2 and Ndd1 (Horak, 2002; Pramila *et al*, 2002, 2006; Darieva *et al*, 2010) and by extension affect expression of the *CLB2* cluster genes that are regulated by Fkh2/Ndd1. To our surprise, expression of the *CLB2* cluster was largely unaffected in cells carrying all 4 Cdk- alleles (Fig 3G). The most likely explanation for this finding is that redundant factors enforce the expression of this group of genes. In support of this possibility, both Fkh2 and Ndd1 are themselves activated by Cdk1 (Reynolds, 2003; Pic-Taylor *et al*, 2004), and this activation still occurs in 4P cells. This regulation fits with our model of how Cdk1 promotes the expression of late cell cycle genes (Fig 8). In combination with previous work, our results suggest that from S-phase through the beginning of mitosis, Cdk1 stimulates the activity of transcriptional activators (Hcm1, Fkh2, Ndd1) and shuts off the activity of transcriptional repressors (Yox1, Yhp1), and together this coordinated regulation drives expression of genes with key mitotic functions. In the future, it will be of interest to determine whether this model applies to regulation by Cdk1 in other systems.

This theme of coordinated positive and negative regulation by Cdk1 not only occurs on the level of the TF network, but also happens on an individual protein. Remarkably, we find that separable Cdk1 sites on Hcm1 mediate its activity and degradation. This raises the possibility that these phosphorylation events may be separated in time: The C-terminal phosphosites of Hcm1 may be phosphorylated first, promoting its activity, followed by phosphorylation of the N-terminal sites to promote its degradation. Conceivably, this could be achieved if the S-phase cyclin/Cdk preferentially phosphorylates the C-terminal sites. Alternatively all sites might be phosphorylated simultaneously, which would result in a limited window of expression of active, but unstable, Hcm1. In either scenario, our data reveal the importance of regulating both the activation and degradation of Hcm1. We found that cells expressing Cdk- Hcm1 are hypersensitive to spindle poisons (Figs 5F and 6B) and are considerably less fit than wild-type cells (Fig 7C). Interestingly, we also found that cells constitutively expressing stable Hcm1 are also hypersensitive to spindle poisons (Fig 5F). Therefore, degradation of Hcm1 plays an important role in tuning the response of the cell to problems that arise with the mitotic spindle.

In contrast, Cdk1 phosphorylation leads to a decrease in the activities of the transcriptional repressors Yox1 and Yhp1. At M/G1 promoters, Yox1 and Yhp1 repress transcription by binding alongside Mcm1 at Early Cell cycle Box (ECB) elements. Interestingly, a recent study suggested that Yox1 and the transcriptional activator Bck2 compete for access to Mcm1 at these promoters (Bastajian *et al*, 2013). Cdk1-mediated phosphorylation of Yox1 might lead to its release from these sites, which could then allow Bck2 to bind and activate transcription. Although our data support the model that Cdk1 limits the activities of Yox1 and Yhp1 by simply promoting their degradation, we cannot rule out the possibility that phosphorylation may also regulate their DNA binding affinities or their interaction with co-regulatory proteins.

In conclusion, we have taken a genetic approach to understand how Cdk1 regulates S-phase TFs *in vivo*. Systematic combination of gene deletions in yeast has led to a wealth of information about how genes and proteins interact in cells (Tong *et al*, 2004; Costanzo *et al*, 2010). To our knowledge, no similar large-scale genetic analysis has been carried out using phospho-deficient alleles of proteins. Our work suggests that this type of approach could be extremely valuable when studying a kinase such as Cdk1 that targets a significant fraction of the proteome (Ubersax *et al*, 2003; Holt *et al*, 2009). By eliminating phosphorylation of a group of TFs that were predicted to act together in a common process, and to be coordinately phosphorylated, we were able to elucidate the specific role of Cdk1 in controlling the late cell cycle transcriptional network and to uncover the importance of this coordinate regulation. In the future, it will be of great interest to test whether unrelated Cdk1 targets with different cellular functions exhibit similar, coordinate regulation. In addition, it will be important to determine whether these general principles of regulation by Cdk1 are conserved in other systems. Coordinated positive and negative regulation by key regulatory kinases may be a conserved mechanism that functions to coordinate diverse processes in response to specific biological or environmental signals.

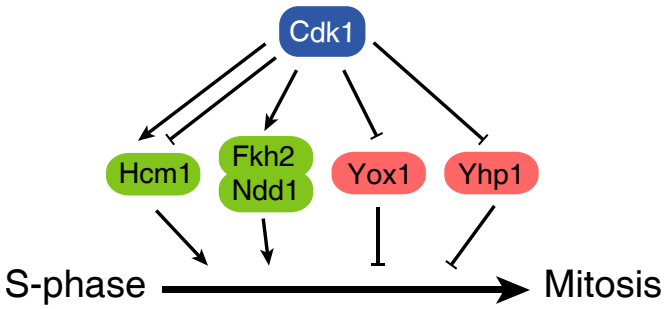

Figure 8. Model of regulation of the late cell cycle gene regulatory network by Cdk1.
See text for details.

Materials and Methods

Yeast strains and plasmids

A complete list of strains, including the specific figures each was used in, is provided in Supplementary Table S1. 3HA-tagged

Cdk- alleles and *HCM1* phosphomimetic alleles were generated by gene synthesis (Biobasic; Invitrogen) and subcloned, along with wild-type counterparts, into the vector pRS413-*GAL1*p. Strains carrying mutations in phosphorylation sites were generated by integrating a PCR product containing the desired mutations, the 3HA tag, and the *HIS3MX* marker at the genomic locus. The integration of each mutation was then confirmed by sequencing. Alternate tags were then added to wild-type and Cdk- genes, as indicated, by replacing the *3HA-HIS3MX* sequence with alternate tag-marker sequences. The 4P strain (containing all four Cdk- alleles) was generated by crossing strains that each carried two phosphomutant alleles and recovering strains carrying all combinations of alleles.

The *TEF1* promoter was introduced upstream of *HCM1* by integration of the *Hyg-TEF1p* cassette directly upstream of the *HCM1* start codon. To construct the *HCM1(1-107)*-GFP strain, *YDR071W* (an uncharacterized, non-essential gene) was replaced in the YDR071W-GFP strain from the GFP collection (Huh *et al*, 2003) with the *Hyg-TEF1p-HCM1(1-107)* sequence. *Hyg-TEF1p-HCM1(1-107)-GFP* was then introduced into the *cdc53-1* background by a genetic cross.

All strains were grown in YM-1 complete medium with 2% dextrose, with the exception of strains carrying plasmids, which were grown in C medium lacking histidine with 2% dextrose or raffinose (Benanti *et al*, 2007). To arrest cells in G1, 20 μg/ml alpha-factor (United Biochemical Research, Inc.) was added for 2–3 h. To arrest cells in mitosis, 10 μg/ml nocodazole (US Biological) was added to cells for 2 h. To arrest cells in early S-phase, 200 mM hydroxyurea (Sigma) was added to cells for 2 h. For G1 arrest-release experiments, cells were arrested in G1 as described above, pelleted, washed once with YM-1, and resuspended in YM-1 with 2% dextrose. Strains carrying temperature-sensitive *CDC53* were grown at 23°C, then shifted to for 2 h (Fig 2E–H), or arrested in nocodazole for 2 h and then shifted to 37°C for 15 min (Fig 5E). Cells carrying the *cdc28-as1* were treated with 5 μM 1NM-PP1 for the indicated amount of time to inhibit Cdk1 activity.

Cell cycle analysis

In all experiments, cell cycle positions were confirmed by flow cytometry. Cells were fixed and labeled with Sytox Green (Invitrogen) as previously described (Landry *et al*, 2012). Samples were analyzed using a FACScan (Becton Dickinson) and data analyzed with FlowJo (Tree Star, Inc.) software.

Western blotting

Equivalent optical densities of cells were collected and lysed as previously described (Landry *et al*, 2012), with the exception of the experiments presented in Figs 1A and D–G, and 2A-I. In these experiments, cell pellets were lysed in cold TCA buffer (10 mM Tris pH 8.0, 10% trichloroacetic acid, 25 mM ammonium acetate, 1 mM EDTA). After incubation on ice, lysates were then centrifuged and the pellets resuspended in resuspension solution (0.1 M Tris pH 11.0, 3% SDS). Samples were heated to 95°C for 5 min, allowed to cool to room temperature, and clarified by centrifugation. Supernatants were added to 4× SDS–PAGE Sample Buffer (0.25 M Tris pH 6.8, 8% SDS, 40% glycerol, 20% β-mercaptoethanol) and heated to 95°C for 5 min. Western blotting was performed as previously described (Landry *et al*, 2012) with antibodies against Myc (Clone 9E10; Covance) Cdc28 (Cdk1) (sc-6709; Santa Cruz Biotechnology), Clb2 (sc-9071; Santa Cruz Biotechnology), Flag (Clone M2; Sigma), HA (Clone 16B12; Covance), V5 (Invitrogen), GFP (Clone JL8; Clontech). Where indicated, protein levels were quantified using ImageJ and normalizing to Cdk1 as a loading control.

Kinase assays

Strains expressing 3HA-tagged WT or Cdk- TFs from the *GAL1* promoter on a plasmid were arrested in G1 with alpha-factor (when Cdk1 activity is low), and expression was induced by the addition of galactose. TFs were immunoprecipitated with anti-HA antibody (clone 12CA5 or 16B12) bound to magnetic protein A or G beads and phoshphorylated with Clb2/Cdk1 kinase that had been purified as previously described (Lopez-Mosqueda *et al*, 2010). Cold kinase reactions (Fig 1B) were carried out in reaction buffer (25 mM Hepes-OH pH 8, 15 mM NaCl, 1 mM $MgCl_2$, 1 mM DTT, 1 mM ATP) with Clb2/Cdk1 kinase for 45 min at room temperature, and phosphorylation was assayed by Western blot. Radioactive kinase assays (Supplementary Fig S1B) were carried out in similar buffer (25 mM Hepes-OH pH 8, 15 mM NaCl, 1 mM $MgCl_2$, 1 mM DTT, 20 μM ATP) supplemented with γ-^{32}P-ATP, and assayed by SDS–PAGE followed by autoradiography. Phosphorylation of Yox1 and Hcm1 mutants were quantified using a GE Typhoon 9000 phosphorimager and ImageJ software.

Cycloheximide-chase assays

Cells were grown to mid-log phase, or arrested as indicated, and assays carried out as previously described (Landry *et al*, 2012).

Microarray analysis

RNA was purified as described (Schmitt *et al*, 1990). One to 5 μg of total RNA was then subjected to RNA amplification and labeling using the Low Input Quick Amp Labeling Kit protocol (Agilent) with minor modifications. Briefly, cRNA was amplified by *in vitro* transcription with amino-allyl UTP (3:2 ratio for amino-ally UTP: UTP) overnight at 37°C. Then, cRNA was purified using RNA Clean and Concentrator columns (Zymo Research) and labeled with Cy3 or Cy5 (GE Healthcare) at room temperature for 90 min in the dark. The fluorescence intensities of Cy3 and Cy5 were determined by NanoDrop, and 600 ng of each cRNA was used for fragmentation and hybridization on Agilent Yeast (V2) Gene Expression Microarrays, 8 × 15 K. Slides were scanned on Agilent DNA microarray scanner G2565CA, and fluorescence data were obtained using Agilent Feature Extraction software at the UMass Medical School genomics core facility. The microarray data from this publication have been submitted to the Gene Expression Omnibus database (http://www.ncbi.nlm.nih.gov/geo/) and assigned the identifier GSE55121.

RT-qPCR

RNA was digested with DNaseI (New England Biolabs) and precipitated. One to 2 μg of RNA was then reverse-transcribed using Random Primers (Invitrogen), followed by digestion with RNaseH

(New England Biolabs). For qPCR, RT samples were mixed with 2× SYBR Fast Master Mix Universal (Kapa Biosystems) and indicated primers (Supplementary Table S2), and reactions were carried out on a Mastercycler ep realplex (Eppendorf) or a Roche LightCycler 96. mRNA levels for each sample were calculated by first subtracting any signal from the no reverse transcriptase control reactions and then normalizing each value to corresponding value for *ACT1*. Fold change was calculated by comparing to mRNA levels in wild-type cells.

Serial dilution assays

Cells were grown to mid-log phase, and fivefold dilutions were plated on rich media plates with 2% dextrose (YPD), rich media plates with 2% dextrose and benomyl, synthetic complete plates lacking histidine with 2% dextrose, or synthetic complete plates lacking histidine with 2% galactose and incubated at 30°C. Plates were removed from the incubator when colony sizes of control strains were comparable.

Chromatin immunoprecipitation

Equivalent optical densities of cells were fixed using 1/10 volume of fix solution (11% formaldehyde, 0.1 M NaCl, 1 mM EDTA, 50 mM HEPES-KOH pH 7.6) for 10 min and the reaction was then quenched by the addition of 1/5 volume 2.5 M glycine for 5 min. Cells were pelleted, washed twice with cold TBS and lysed in 1× Lysis Buffer (25 mM HEPES-KOH pH7.6, 400 mM NaCl, 0.2% Triton X-100, 1 mM EDTA, 10% glycerol, 1 μg/ml leupeptin, 1 μg/ml bestatin, 1 mM benzamidine, 1 μg/ml pepstatin A, 17 μg/ml PMSF, 5 mM sodium fluoride, 80 mM β-glycerophosphate and 1 mM sodium orthovanadate) by bead beating cold for 5 min. Cell lysates were washed three times with FA Buffer + PIC (50 mM HEPES-KOH pH 7.6, 150 mM NaCl, 1 mM EDTA, 1% Triton X-100, 0.1% Na deoxycholate, 1 μg/ml leupeptin, 1 μg/ml bestatin, 1 mM benzamidine, 1 μg/ml pepstatin A, 17 μg/ml PMSF, 5 mM sodium fluoride, 80 mM β-glycerophosphate, and 1 mM sodium orthovanadate), resuspended in 1 ml FA Buffer + PIC, and sonicated in a Bioruptor (UCD-200) for 30 min. Cell lysates were centrifuged and supernatant was transferred to a new tube, a fraction of the lysate was aliquotted into 2× Stop Buffer (20 mM Tris-HCl pH 8.0, 100 mM NaCl, 20 mM EDTA, 1% SDS), and the remainder incubated overnight with magnetic beads pre-coupled to the specified antibody. Lysates were then washed 2× with ChIP Buffer + PIC (20 mM Tris-HCl pH 8.0, 150 mM NaCl, 2 mM EDTA, 1% Triton X-100, 1 μg/ml leupeptin, 1 μg/ml bestatin, 1 mM benzamidine), 2× with High Salt ChIP Buffer + PIC (20 mM Tris-HCl pH 8.0, 650 mM NaCl, 2 mM EDTA, 1% Triton X-100, 1 μg/ml leupeptin, 1 μg/ml bestatin, 1 mM benzamidine), and 4× with RIPA Buffer (10 mM Tris-HCl pH 8.0, 0.25 M LiCl, 1 mM EDTA, 0.5% NP-40, 0.5% Na deoxycholate). Cross-linking was reversed by mixing at 65°C for 30 min in 2× Stop Buffer. 200 μl TE was added to lysates and samples were treated with Proteinase K for 4 h at 65°C. Samples were then phenol:chloroform: isoamyl alcohol extracted using phase-lock tubes. Chromatin was resuspended in 10 mM Tris-HCl pH 8.0 + 1 μg/ml RNase A and incubated at 37°C for 20 min. qPCR was then performed as described above compared to a dilution series made from the input DNA as the standard curve. Primers are listed in Supplementary Table S2.

Cell size measurements

Cells were grown to mid-log phase and measured on a Beckman Coulter Multisizer 3 Coulter Counter. Median size measurements were calculated using the Beckman Coulter Particle Characterization software version 3.53.

Competition assays

Competition assays were carried out as previously described (Torres *et al*, 2010). Equal numbers of cells with and without *PGK1-GFP* were co-cultured in 10 ml YM-1 with 20% dextrose and diluted every 12 h to keep cultures in continuous exponential growth phase. Cells were fixed in ethanol at the indicated time points and quantified after the completion of the experiment using a FACScan (Becton Dickinson). Data were analyzed with FlowJo (Tree Star, Inc.) software.

Supplementary information for this article is available online: http://emboj.embopress.org

Acknowledgments

We thank Eduardo Torres for technical help and for assistance in analyzing microarray data. We also thank Tyler Doughty, Tom Fazzio, Peter Pryciak, and David Toczyski for valuable discussions and critical reading of the manuscript. This work was supported by National Institutes of Health Grant R00GM085013 and the Richard and Susan Smith Family Foundation. The funders had no role in study design, data collection and analysis, decision to publish, or preparation of the manuscript.

Author contributions

JAB and BDL designed the experiments. BDL, HEA, CEM, and KEP carried out the experiments. JAB, BDL, HEA, and CEM analyzed the data. JAB wrote the paper.

Conflict of interest

The authors declare that they have no conflict of interest.

References

Agarwal R, Tang Z, Yu H, Cohen-Fix O (2003) Two distinct pathways for inhibiting pds1 ubiquitination in response to DNA damage. *J Biol Chem* 278: 45027 – 45033

Bastajian N, Friesen H, Andrews BJ (2013) Bck2 acts through the MADS box protein Mcm1 to activate cell-cycle-regulated genes in budding yeast. *PLoS Genet* 9: e1003507

Benanti JA (2012) Coordination of cell growth and division by the ubiquitin-proteasome system. *Semin Cell Dev Biol* 23: 492 – 498

Benanti JA, Cheung SK, Brady MC, Toczyski DP (2007) A proteomic screen reveals SCFGrr1 targets that regulate the glycolytic-gluconeogenic switch. *Nat Cell Biol* 9: 1184 – 1191

Bertoli C, Skotheim JM, de Bruin RAM (2013) nrm3629. *Nat Rev Mol Cell Biol* 14: 518 – 528

de Bruin RAM, McDonald WH, Kalashnikova TI, Yates J, Wittenberg C (2004) Cln3 activates G1-specific transcription via phosphorylation of the SBF bound repressor Whi5. *Cell* 117: 887 – 898

Cho RJ, Campbell MJ, Winzeler EA, Steinmetz L, Conway A, Wodicka L, Wolfsberg TG, Gabrielian AE, Landsman D, Lockhart DJ, Davis RW (1998) A

genome-wide transcriptional analysis of the mitotic cell cycle. *Mol Cell* 2: 65–73

Costanzo M, Baryshnikova A, Bellay J, Kim Y, Spear ED, Sevier CS, Ding H, Koh JLY, Toufighi K, Mostafavi S, Prinz J, St Onge RP, VanderSluis B, Makhnevych T, Vizeacoumar FJ, Alizadeh S, Bahr S, Brost RL, Chen Y, Cokol M *et al* (2010) The genetic landscape of a cell. *Science* 327: 425–431

Costanzo M, Nishikawa JL, Tang X, Millman JS, Schub O, Breitkreuz K, Dewar D, Rupes I, Andrews B, Tyers M (2004) CDK activity antagonizes Whi5, an inhibitor of G1/S transcription in yeast. *Cell* 117: 899–913

Cross FR, Buchler NE, Skotheim JM (2011) Evolution of networks and sequences in eukaryotic cell cycle control. *Philos Trans R Soc Lond B Biol Sci* 366: 3532–3544

Daniel JA, Keyes BE, Ng YPY, Freeman CO, Burke DJ (2006) Diverse functions of spindle assembly checkpoint genes in *Saccharomyces cerevisiae*. *Genetics* 172: 53–65

Darieva Z, Clancy A, Bulmer R, Williams E, Pic-Taylor A, Morgan BA, Sharrocks AD (2010) A competitive transcription factor binding mechanism determines the timing of late cell cycle-dependent gene expression. *Mol Cell* 38: 29–40

Haase SB, Reed SI (1999) Evidence that a free-running oscillator drives G1 events in the budding yeast cell cycle. *Nature* 401: 394–397

Haase SB, Wittenberg C (2014) Topology and control of the cell-cycle-regulated transcriptional circuitry. *Genetics* 196: 65–90

Hao B, Oehlmann S, Sowa ME, Harper JW, Pavletich NP (2007) Structure of a Fbw7-Skp1-cyclin E complex: multisite-phosphorylated substrate recognition by SCF ubiquitin ligases. *Mol Cell* 26: 131–143

Henley SA, Dick FA (2012) The retinoblastoma family of proteins and their regulatory functions in the mammalian cell division cycle. *Cell Div* 7: 10

van den Heuvel S, Dyson NJ (2008) Conserved functions of the pRB and E2F families. *Nat Rev Mol Cell Biol* 9: 713–724

Holt LJ, Krutchinsky AN, Morgan DO (2008) Positive feedback sharpens the anaphase switch. *Nature* 454: 353–357

Holt LJ, Tuch BB, Villén J, Johnson AD, Gygi SP, Morgan DO (2009) Global analysis of Cdk1 substrate phosphorylation sites provides insights into evolution. *Science* 325: 1682–1686

Horak CE, Luscombe NM, Qian J, Bertone P, Piccirrillo S, Gerstein M, Snyder M (2002) Complex transcriptional circuitry at the G1/S transition in Saccharomyces cerevisiae. *Genes Dev* 16: 3017–3033

Horak J (2002) Two distinct proteolytic systems responsible for glucose-induced degradation of fructose-1,6-bisphosphatase and the Gal2p transporter in the yeast *Saccharomyces cerevisiae* share the same protein components of the glucose signaling pathway. *J Biol Chem* 277: 8248–8254

Huh W-K, Falvo JV, Gerke LC, Carroll AS, Howson RW, Weissman JS, O'Shea EK (2003) Global analysis of protein localization in budding yeast. *Nature* 425: 686–691

Jorgensen P, Nishikawa JL, Breitkreutz B-J, Tyers M (2002) Systematic identification of pathways that couple cell growth and division in yeast. *Science* 297: 395–400

Kõivomägi M, Valk E, Venta R, Iofik A, Lepiku M, Balog ERM, Rubin SM, Morgan DO, Loog M (2011a) Cascades of multisite phosphorylation control Sic1 destruction at the onset of S phase. *Nature* 480: 128–131

Kõivomägi M, Valk E, Venta R, Iofik A, Lepiku M, Morgan DO, Loog M (2011b) Dynamics of Cdk1 substrate specificity during the cell cycle. *Mol Cell* 42: 610–623

Koranda M, Schleiffer A, Endler L, Ammerer G (2000) Forkhead-like transcription factors recruit Ndd1 to the chromatin of G2/M-specific promoters. *Nature* 406: 94–98

Kumar R, Reynolds DM, Shevchenko A, Shevchenko A, Goldstone SD, Dalton S (2000) Forkhead transcription factors, Fkh1p and Fkh2p, collaborate with Mcm1p to control transcription required for M-phase. *Curr Biol* 10: 896–906

Landry BD, Doyle JP, Toczyski DP, Benanti JA (2012) F-box protein specificity for G1 cyclins is dictated by subcellular localization. *PLoS Genet* 8: e1002851

Lanker S, Valdivieso MH, Wittenberg C (1996) Rapid degradation of the G1 cyclin Cln2 induced by CDK-dependent phosphorylation. *Science* 271: 1597–1601

Laoukili J, Alvarez M, Meijer LAT, Stahl M, Mohammed S, Kleij L, Heck AJR, Medema RH (2008) Activation of FoxM1 during G2 requires cyclin A/Cdk-dependent relief of autorepression by the FoxM1 N-terminal domain. *Mol Cell Biol* 28: 3076–3087

Laoukili J, Kooistra MRH, Brás A, Kauw J, Kerkhoven RM, Morrison A, Clevers H, Medema RH (2005) FoxM1 is required for execution of the mitotic programme and chromosome stability. *Nat Cell Biol* 7: 126–136

Littlepage LE, Ruderman JV (2002) Identification of a new APC/C recognition domain, the A box, which is required for the Cdh1-dependent destruction of the kinase Aurora-A during mitotic exit. *Genes Dev* 16: 2274–2285

Loog M, Morgan DO (2005) Cyclin specificity in the phosphorylation of cyclin-dependent kinase substrates. *Nature* 434: 104–108

Lopez-Mosqueda J, Maas NL, Jonsson ZO, Defazio-Eli LG, Wohlschlegel J, Toczyski DP (2010) Damage-induced phosphorylation of Sld3 is important to block late origin firing. *Nature* 467: 479–483

Loy CJ, Lydall D, Surana U (1999) NDD1, a high-dosage suppressor of cdc28-1N, is essential for expression of a subset of late-S-phase-specific genes in *Saccharomyces cerevisiae*. *Mol Cell Biol* 19: 3312–3327

Lu Y, Mahony S, Benos PV, Rosenfeld R, Simon I, Breeden LL, Bar-Joseph Z (2007) Combined analysis reveals a core set of cycling genes. *Genome Biol* 8: R146

Lüscher-Firzlaff JM, Lilischkis R, Lüscher B (2006) Regulation of the transcription factor FOXM1c by Cyclin E/CDK2. *FEBS Lett* 580: 1716–1722

Lyons NA, Fonslow BR, Diedrich JK, Yates JR, Morgan DO (2013) Sequential primed kinases create a damage-responsive phosphodegron on Eco1. *Nat Struct Mol Biol* 20: 194–201

Mailand N, Diffley JFX (2005) CDKs promote DNA replication origin licensing in human cells by protecting Cdc6 from APC/C-dependent proteolysis. *Cell* 122: 915–926

Major ML, Lepe R, Costa RH (2004) Forkhead box M1B transcriptional activity requires binding of Cdk-cyclin complexes for phosphorylation-dependent recruitment of p300/CBP coactivators. *Mol Cell Biol* 24: 2649–2661

Massagué J (2004) G1 cell-cycle control and cancer. *Nature* 432: 298–306

Morgan DO (2007) *The Cell Cycle*. London: New Science Press

Myatt SS, Lam EWF (2007) The emerging roles of forkhead box (Fox) proteins in cancer. *Nat Rev Cancer* 7: 847–859

Nash P, Tang X, Orlicky S, Chen Q, Gertler FB, Mendenhall MD, Sicheri F, Pawson T, Tyers M (2001) Multisite phosphorylation of a CDK inhibitor sets a threshold for the onset of DNA replication. *Nature* 414: 514–521

de Oliveira FMB, Harris MR, Brazauskas P, de Bruin RAM, Smolka MB (2012) Linking DNA replication checkpoint to MBF cell-cycle transcription reveals a distinct class of G1/S genes. *EMBO J* 31: 1798–1810

Orlando DA, Lin CY, Bernard A, Wang JY, Socolar JES, Iversen ES, Hartemink AJ, Haase SB (2008) Global control of cell-cycle transcription by coupled CDK and network oscillators. *Nature* 453: 944–947

Ostapenko D, Ostapenko D, Burton JL, Burton JL, Solomon MJ, Solomon MJ (2012) Identification of Anaphase Promoting Complex Substrates in

S. cerevisiae. *PLoS One* 7: e45895. Available at: http://dx.plos.org/10.1371/journal.pone.0045895.g006

Ostapenko D, Solomon MJ (2011) Anaphase promoting complex-dependent degradation of transcriptional repressors Nrm1 and Yhp1 in *Saccharomyces cerevisiae*. *Mol Biol Cell* 22: 2175–2184

Pic A, Lim FL, Ross SJ, Veal EA, Johnson AL, Sultan MR, West AG, Johnston LH, Sharrocks AD, Morgan BA (2000) The forkhead protein Fkh2 is a component of the yeast cell cycle transcription factor SFF. *EMBO J* 19: 3750–3761

Pic-Taylor A, Darieva Z, Morgan BA, Sharrocks AD (2004) Regulation of cell cycle-specific gene expression through cyclin-dependent kinase-mediated phosphorylation of the Forkhead transcription factor Fkh2p. *Mol Cell Biol* 24: 10036–10046

Pramila T, Miles S, GuhaThakurta D, Jemiolo D, Breeden LL (2002) Conserved homeodomain proteins interact with MADS box protein Mcm1 to restrict ECB-dependent transcription to the M/G1 phase of the cell cycle. *Genes Dev* 16: 3034–3045

Pramila T, Wu W, Miles S, Noble WS, Breeden LL (2006) The Forkhead transcription factor Hcm1 regulates chromosome segregation genes and fills the S-phase gap in the transcriptional circuitry of the cell cycle. *Genes Dev* 20: 2266–2278

Reynolds D (2003) Recruitment of Thr 319-phosphorylated Ndd1p to the FHA domain of Fkh2p requires Clbkinase activity: a mechanism for CLB cluster gene activation. *Genes Dev* 17: 1789–1802

Schmitt ME, Brown TA, Trumpower BL (1990) A rapid and simple method for preparation of RNA from *Saccharomyces cerevisiae*. *Nucleic Acids Res* 18: 3091–3092

Shevchenko A, Roguev A, Schaft D, Buchanan L, Habermann B, Sakalar C, Thomas H, Krogan NJ, Shevchenko A, Stewart AF (2008) Chromatin Central: towards the comparative proteome by accurate mapping of the yeast proteomic environment. *Genome Biol* 9: R167

Simmons Kovacs LA, Mayhew MB, Orlando DA, Jin Y, Li Q, Huang C, Reed SI, Mukherjee S, Haase SB (2012) Cyclin-dependent kinases are regulators and effectors of oscillations driven by a transcription factor network. *Mol Cell* 45: 669–679

Skaar JR, Pagan JK, Pagano M (2013) Mechanisms and function of substrate recruitment by F-box proteins. *Nat Rev Mol Cell Biol* 14: 369–381

Spellman PT, Sherlock G, Zhang MQ, Iyer VR, Anders K, Eisen MB, Brown PO, Botstein D, Futcher B (1998) Comprehensive identification of cell cycle-regulated genes of the yeast *Saccharomyces cerevisiae* by microarray hybridization. *Mol Biol Cell* 9: 3273–3297

Strickfaden SC, Winters MJ, Ben-Ari G, Lamson RE, Tyers M, Pryciak PM (2007) A mechanism for cell-cycle regulation of MAP kinase signaling in a yeast differentiation pathway. *Cell* 128: 519–531

Thornton BR, Toczyski DP (2003) Securin and B-cyclin/CDK are the only essential targets of the APC. *Nat Cell Biol* 5: 1090–1094

Tong AHY, Lesage G, Bader GD, Ding H, Xu H, Xin X, Young J, Berriz GF, Brost RL, Chang M, Chen Y, Cheng X, Chua G, Friesen H, Goldberg DS, Haynes J, Humphries C, He G, Hussein S, Ke L *et al* (2004) Global mapping of the yeast genetic interaction network. *Science* 303: 808–813

Torres EM, Dephoure N, Panneerselvam A, Tucker CM, Whittaker CA, Gygi SP, Dunham MJ, Amon A (2010) Identification of aneuploidy-tolerating mutations. *Cell* 143: 71–83

Ubersax JA, Woodbury EL, Quang PN, Paraz M, Blethrow JD, Shah K, Shokat KM, Morgan DO (2003) Targets of the cyclin-dependent kinase Cdk1. *Nature* 425: 859–864

Wierstra I, Alves J (2006) FOXM1c is activated by cyclin E/Cdk2, cyclin A/Cdk2, and cyclin A/Cdk1, but repressed by GSK-3alpha. *Biochem Biophys Res Commun* 348: 99–108

Willems AR, Schwab M, Tyers M (2004) A hitchhiker's guide to the cullin ubiquitin ligases: SCF and its kin. *Biochim Biophys Acta* 1695: 133–170

Zachariae W, Schwab M, Nasmyth K, Seufert W (1998) Control of cyclin ubiquitination by CDK-regulated binding of Hct1 to the anaphase promoting complex. *Science* 282: 1721–1724

Zhu G, Spellman PT, Volpe T, Brown PO, Botstein D, Davis TN, Futcher B (2000) Two yeast forkhead genes regulate the cell cycle and pseudohyphal growth. *Nature* 406: 90–94

